Self-tuning bistable parametric feedback oscillator: Near-optimal amplitude maximization without model information

David J. Braun,[1,*] Andrius Sutas,[2] and Sethu Vijayakumar[2]
[1]*Singapore University of Technology and Design, 8 Somapah Road, 487372 Singapore*
[2]*The University of Edinburgh, 10 Crichton Street, Edinburgh EH8 9AB, United Kingdom*
(Received 8 May 2016; published 3 January 2017)

Theory predicts that parametrically excited oscillators, tuned to operate under resonant condition, are capable of large-amplitude oscillation useful in diverse applications, such as signal amplification, communication, and analog computation. However, due to amplitude saturation caused by nonlinearity, lack of robustness to model uncertainty, and limited sensitivity to parameter modulation, these oscillators require fine-tuning and strong modulation to generate robust large-amplitude oscillation. Here we present a principle of self-tuning parametric feedback excitation that alleviates the above-mentioned limitations. This is achieved using a minimalistic control implementation that performs (i) self-tuning (slow parameter adaptation) and (ii) feedback pumping (fast parameter modulation), without sophisticated signal processing past observations. The proposed approach provides near-optimal amplitude maximization without requiring model-based control computation, previously perceived inevitable to implement optimal control principles in practical application. Experimental implementation of the theory shows that the oscillator self-tunes itself near to the onset of dynamic bifurcation to achieve extreme sensitivity to small resonant parametric perturbations. As a result, it achieves large-amplitude oscillations by capitalizing on the effect of nonlinearity, despite substantial model uncertainties and strong unforeseen external perturbations. We envision the present finding to provide an effective and robust approach to parametric excitation when it comes to real-world application.

DOI: 10.1103/PhysRevE.95.012201

I. INTRODUCTION

Parametric excitation is a way to set oscillators in motion by modulating their physical parameters. There is a characteristic instability effect—known as principal parametric resonance—where oscillations are achieved by parameter modulation that has twice the natural frequency of the oscillator [1,2]. This phenomenon is quite different from the one associated with resonance by forced excitation.

The first well-documented example of a parametrically excited system is the *O Botafumeiro*, a censer suspended by a long rope in the Cathedral of Santiago de Compostela in the northwest region of Spain, which dates back to the 14th century [3]. This giant variable-length pendulum was set into motion by a squat of priests who pulled the rope to cyclically decrease and increase its length at the lowest and highest points of the oscillation until they got the censer to the vaults. The principle of parametric excitation was found useful in different physical domains and various applications [4], such as mechanical domain signal amplification [5], particle traps enabling atomic-level measurements [6], signal amplifiers revealing quantum information [7], nanoelectromechanical oscillators challenging current standard quartz-crystal clocks in timing applications [8], optical calculators performing difficult mathematical calculations [9], as well as networks of electromechanical oscillators promising energy-efficient analog computation [10,11].

An ideal parametrically excited oscillator is operated in the linear regime using time-dependent parameter modulation. The model of such an oscillator is given by Mathieu's equation [12] which predicts an infinite sequence of instability regions [13] defined by the amplitude and frequency of the excitation [14]. According to the theory, the presence of weak dissipation may not limit the amplitude of the motion [15], while addition of parasitic nonlinearity leads to finite amplitude oscillations. This reflects, more closely, the real-world observation [16].

The effect of amplitude saturation inherent to nonlinear vibrations, the sensitivity to model uncertainty (inevitably present in real-world applications), and the limited sensitivity to small parametric perturbations (apparent on most typical monostable oscillators [17]) have been long perceived to limit technological promises of actuation principles that employ system parameter modulation.

In this paper we present a principle of *self-tuning feedback parameter modulation* that is immune to the above-mentioned limitations. Instead of the classical time-dependent parametric excitation, or more recent time-delay feedback-based control implementations [8,18–20], we combine minimalistic statistical information with optimal state feedback control perturbations to realize *self-tuning* (slow autonomous parameter adaptation) and *feedback pumping* (fast state-dependent parameter modulation) without model information, delicate control computation, or sophisticated signal processing past observations.

Similar to most typical parametric feedback excitation schemes, this approach leads to a self-sustained oscillator [21] capable of large-amplitude oscillations. However, unlike alternative means to parameter modulation, it (i) exploits the extreme sensitivity of bistable oscillators near the onset of their dynamic bifurcation [22] and (ii) uses optimal feedback control perturbations [23]. We present the first experimental demonstration of this principle, which is shown to provide unprecedentedly robust amplitude maximization despite weak

*david_braun@sutd.edu.sg

parametric excitation, substantial model variation, and strong unforeseen external perturbations.

II. OPTIMAL PARAMETRIC EXCITATION

A minimalistic model of a nonlinear parametric oscillator is given by

$$\ddot{q} + \gamma\dot{q} + kq + k_3 q^3 = 0, \tag{1}$$

where q denotes the displacement of the oscillator, γ characterizes viscous dissipation, k is the stiffness of the oscillator, while the last term, where $k_3 > 0$, represents Duffing-type nonlinearity [24]. The stiffness of the oscillator can be decomposed into

$$k = k_o + k_p(t), \tag{2}$$

where the first term is the static stiffness while the second term is the dynamic stiffness. When the parameter of the oscillator is not subject to modulation $k_p(t) = 0$, the oscillator can be monostable $k_o > 0$ (characterized with single-well static potential) or bistable $k_o < 0$ (characterized with double-well static potential).

The oscillator (1) can be set into motion by stiffness modulation, i.e., by changing $k_p(t) \in [k_{p\,\min}, k_{p\,\max}]$. For a linear oscillator this can be done using, e.g., square-wave modulation [25], which has twice the frequency of the oscillator and which has an amplitude that exceeds the threshold $k_{p\,\max} - k_{p\,\min} > \pi\sqrt{k_o}\gamma$ defined by the static stiffness and the coefficient of viscous dissipation. This kind of limitation is fundamental to the principle of parametric excitation. It indicates that, in order to generate oscillations, the energy injected through parameter modulation must exceed the energy lost due to dissipation.

Figure 1(a) shows a typical long-term behavior of a nonlinear oscillator (1) under optimal dynamic stiffness modulation $k_p = k_p^{\text{opt}}(t) \in [k_{p\,\min}, k_{p\,\max}]$ and different static stiffness k_o settings. *The implemented time-dependent modulation maximizes the amplitude of the oscillator at every oscillation.* This modulation is the most effective among all modulations subject to the same stiffness range limitation. Despite this, we observe that when the oscillator operates in the monostable regime its amplitude and sensitivity to parameter modulation is limited compared to that observed just before the onset of the dynamic bifurcation (gray area). In addition to this, the implemented time-dependent excitation lacks robustness and the capacity of adaptation vital for robust practical implementation. This is why the benefit offered by model-based optimization diminishes when it comes to real-world implementation.

III. NEAR-OPTIMAL ADAPTIVE FEEDBACK PARAMETRIC EXCITATION

Ideally, we wish to realize effective amplitude maximization that is inherently robust under uncertainties in model information and unforeseen external perturbations. While using a model-based time-dependent (feed-forward) controller this does not seem to be viable, here we propose a minimalistic adaptive feedback controller that implements self-tuning (long-term parameter adaptation) and near-optimal feedback pumping (short-term parameter modulation) without sophisticated model-based control computation. The principles that underly this controller are summarized in the following two observations:

(1) The amplitude of the oscillator is maximized near to the onset of dynamic bifurcation [Fig. 1(a), gray area] where

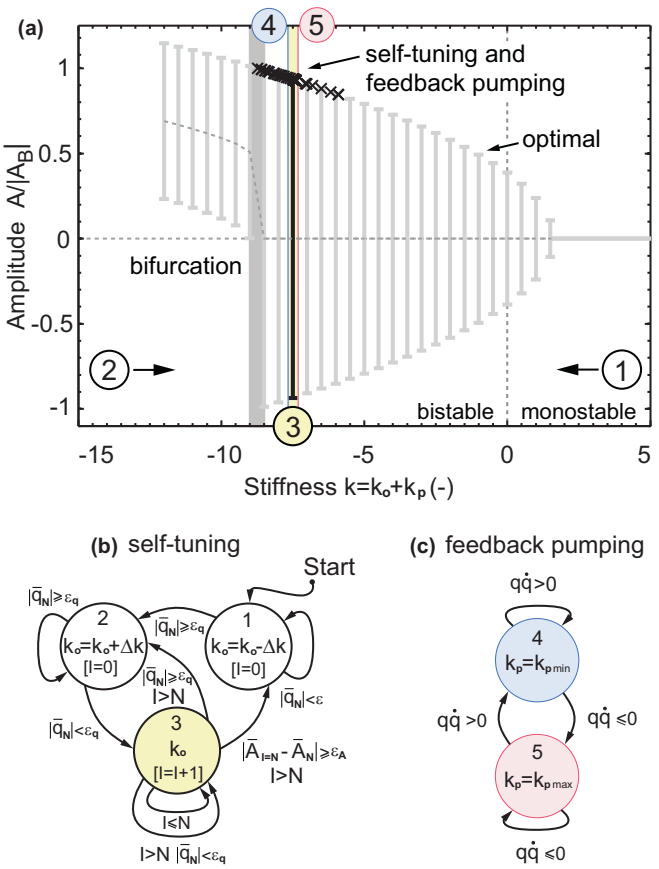

FIG. 1. (a) Model-based optimal parametric excitation. The stationary amplitude A of the oscillator is shown with gray lines. $|A| \approx |A_B|$ denotes the state of the oscillator before the onset of bifurcation (shaded gray area). The model parameters are given by $k_o \in [-12,5]$, $k_p^{\text{opt}}(t) \in [-0.2,0.2]$, $\gamma = 0.1$, and $k_3 = 1$. (b) Model free feedback controller used to tune the oscillator, where $\bar{q}_N$ denotes the $N = 2$ period moving average position, $\bar{A}_N$ is the corresponding average amplitude, $\Delta k = 0.1$ is the stiffness increment per motion cycle, while $\epsilon_q = 0.1$ and $\epsilon_A = 0.01$ denote the two switching thresholds, respectively [26]. (c) Model-free optimal feedback controller used to implement fast parameter modulation. The black dots in subplot (a) represent the operation points of the oscillator after self-tuning. The black line denotes the mean amplitude of the tuned oscillator. The yellow area (state 3) indicates the 99% confidence interval of the tuned static stiffness. These results were obtained by 100 simulations of (1) using random initialization. We note that in the statically monostable regime ($k_0 > 0$) the oscillator could not be always set into motion under the constraint imposed on the amplitude of the fast parameter modulation, i.e., $k_p^{\text{opt}}(t) \in [-0.2,0.2]$. Despite this, the oscillator displays large-amplitude motion after it self-tunes itself near to the onset of dynamic bifurcation (state 3, yellow area).

it displays extreme sensitivity to resonant perturbations [22]. Based on this observation, we aim to adaptively change the stiffness of the oscillator k_o, in order to tune the system near to the onset of its dynamic bifurcation [Fig. 1(a), state 3, yellow area]. This is implemented using simple statistical information—N-period mean position $\bar{q}_N$ and mean amplitude $\bar{A}_N$ of the oscillator—using minimalistic on-line computation and without model information [see Fig. 1(b)]:

$$k_o = k_o(\bar{q}_N, \bar{A}_N). \tag{3}$$

According to this implementation, adaptation is achieved by first reducing stiffness [Fig. 1(b) state 1], in order to induce off-centered motion, and then increasing stiffness [Fig. 1(b) state 2], until the emergence of centered large-amplitude oscillations [Figs. 1(a) and 1(b) state 3, yellow area). There are three important features of this tuning approach: First it is easy to implement (it does not require extensive computation); second, it is model-free (it does not require system parameter identification); and, third, it is robust (it relies on generic features of bistable oscillators) [27]. We now turn to the second observation.

(2) In order to achieve amplitude maximization, the optimal parametric pump implements the following simple actions: Every time the oscillator passes through its trivial equilibrium stiffness is reduced while every time the oscillator reaches its maximum amplitude stiffness is increased [28] [Fig. 1(c)]:

$$k_p(q,\dot{q}) \in \begin{cases} k_{\mathrm{pmax}} & \text{if } q\dot{q} \leqslant 0 \\ k_{\mathrm{pmin}} & \text{if } q\dot{q} > 0. \end{cases} \tag{4}$$

We have recently shown [23] that this feedback controller delivers the same amplification effect as the corresponding model-based optimal excitation which maximizes the amplitude of the oscillator at every oscillation. Importantly, this holds not only for linear oscillators but also for a large class of essentially nonlinear oscillators, including bistable oscillators. In addition to this, this controller does not require model information or control computation and, similarly to other feedback based excitation schemes [8,18–20,29], it is inherently robust compared to time-dependent parametric excitation. These features make (4) desirable when it comes to real-world implementation.

When applied to a prototypical bistable oscillator (1), the composite controller:

$$k = k_o(\bar{q}_N, \bar{A}_N) + k_p(q,\dot{q}) \tag{5}$$

adaptively tunes the system to the onset of its dynamic bifurcation where it achieves large-amplitude parametric oscillations (see Fig. 1). In general, however, application of this controller on more complex oscillators appears to be hindered by two fundamental limitations. This is partly because the stiffness parameter of a real physical systems is, in general, not directly controllable [30] but also because the above controller (5) requires stiffness modulation in two fundamentally different spatial and temporal scales, i.e., while the first term k_o requires large-range and slow cycle-to-cycle adaptation, the second term k_p is designated to small-range but fast stiffness modulation. Due to these reasons, it is often difficult to provide a generalization of the above controller that (i) remains effective in amplitude maximization, (ii) remains robust to model variations, and (iii) enables low-energy-cost practical implementation.

IV. GENERALIZATION AND PRACTICAL IMPLEMENTATION

In this section we present a practical realization of a self-tuning bistable parametric oscillator [Figs. 2(a)–2(c)] which is not affected by the above-mentioned limitations. Using this oscillator, we aim to outline *general design features* that enable effective implementation of the proposed control scheme for parametric excitation.

The behavior of the oscillator is captured by a three-degree-of-freedom model [Fig. 2(d)]:

$$\ddot{q} + \gamma\dot{q} + k(q,\boldsymbol{x})q = 0, \tag{6}$$

$$\ddot{\boldsymbol{x}} + 2\boldsymbol{\alpha}\dot{\boldsymbol{x}} + \boldsymbol{\alpha}^2\boldsymbol{x} = \boldsymbol{\alpha}^2\boldsymbol{u}, \tag{7}$$

composed by a nonlinear oscillator (6) coupled to a *two-degree of freedom* actuating subsystem (7). In this model, $k(q,\boldsymbol{x})$ denotes the state-dependent stiffness of the oscillator, $\boldsymbol{x} = [x_1,x_2]^\top$ is the displacement of the position controlled actuators, $\boldsymbol{\alpha} = \mathrm{diag}[\alpha_1,\alpha_2]$ quantifies the speed (closed-loop bandwidth) of the actuators, while $\boldsymbol{u} = [u_1,u_2]^\top \in [\boldsymbol{u}_{\min},\boldsymbol{u}_{\max}]$ defines the control inputs. The state-dependent stiffness of this device has additive structure:

$$k(q,\boldsymbol{x}) = k_{\mathrm{I}}(q,x_1) + k_{\mathrm{II}}(q,x_2) + k_{\mathrm{III}}(q), \tag{8}$$

due to the parallel coupling of the three compliant subsystems [Figs. 2(a)–2(d) (I)–(III)]. The first two terms in the above relation are associated with the two leaf-spring mechanisms [Figs. 2(a)–2(d) (I) and (II)]. The stiffness provided by these mechanisms—$k_{\mathrm{I,II}}(q,x_*) \propto (\delta_* + x_{*\max} - x_*)^{-3}[1 - \mathcal{O}(q^2)]$ (where δ_* defines the largest achievable stiffness) [31]—can be changed by controlling the effective length of the leaf springs. In this way, the two actuators are used to change $k_{\mathrm{I,II}}$ from near-zero ($x_* \approx x_{*\min}$, long spring) to high positive values ($x_* \approx x_{*\max}$, short spring). The additional extension spring mechanism is shown in Fig. 2(c) (III). This mechanism is pre-extended in order to pull the oscillator away from its equilibrium configuration ($q = 0$). This effect leads to the third term $k_{\mathrm{III}}(q) \propto -1 + \mathcal{O}(q^2)$ in (8). This term is negative.

The redundancy in actuation (i.e., two independent inputs $\boldsymbol{u} \in \mathbb{R}^2$ are used to change the stiffness $k \in \mathbb{R}$ of the oscillator), the inverse relation between $k_{\mathrm{I,II}}$ and the positions of the actuators $\boldsymbol{x}$, and the instability of the static equilibrium position caused by the negative stiffness element in the oscillator $k_{\mathrm{III}} < 0$ are the three design feature that make this oscillator: wide-range tunable (tunable over monostable to strongly nonlinear bistable regimes [shown in Fig. 2 and Fig. 4]) and well suited to low-power-cost stiffness modulation [see Figs. 2(g) and 2(i) and Fig. 3].

The model presented above (6)–(8) will be subsequently used to explain the working principle of the oscillator. It is, however, important to note that this model is not general enough to perform model-based optimization [32].

Using the actuators (7), we modify the internal geometry of the device to implement redundant parametric excitation. Specifically, we employ a slow actuator u_1 to modulate the

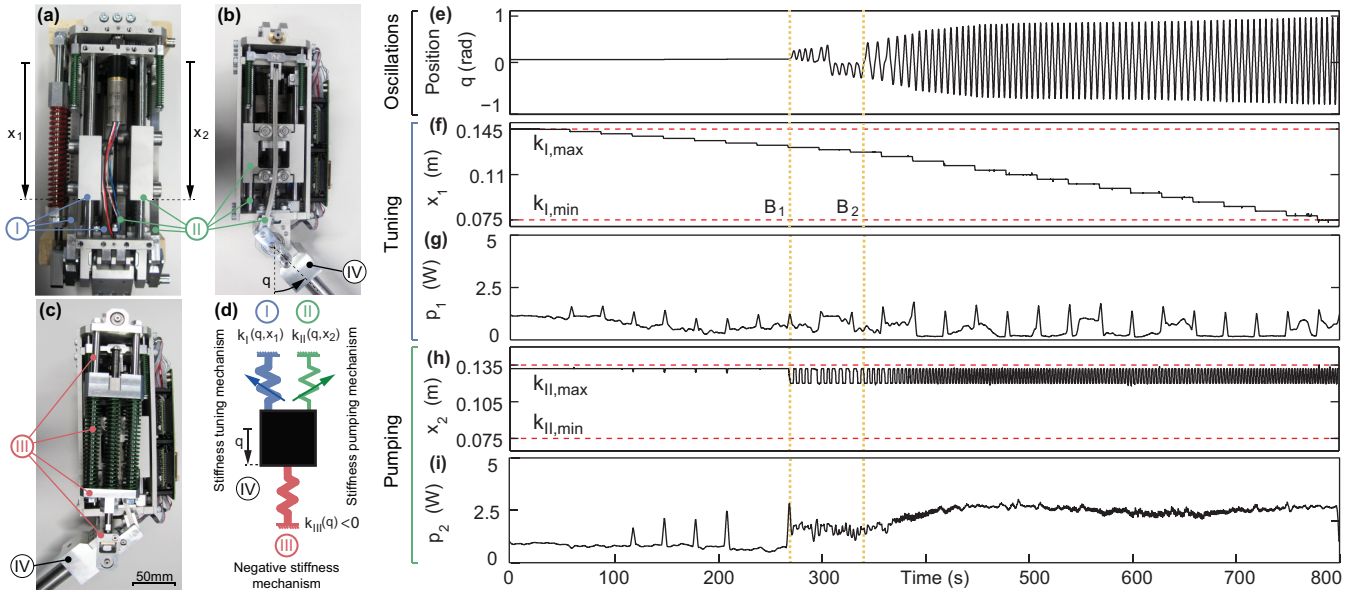

FIG. 2. Tunable parametric feedback oscillator. [(a)–(c)] Oscillator: (I) leaf-spring mechanism dedicated to tuning, (II) leaf-spring mechanism dedicated to feedback pumping, (III) passive positive feedback mechanism, (IV) oscillating output link. (d) Schematic representation of the oscillator. (e) Behavior of the oscillator under (f) quasistatic stiffness tuning and (h) parametric feedback pumping. $B_{1,2}$ denote dynamic bifurcations as the stiffness of the oscillator is decreased. [(g) and (i)] Average electrical power drained by the slow stiffness tuning and the fast stiffness pumping motors (computed using 2.5-s and 0.25-s moving average filters, respectively).

effective length of the first leaf spring x_1 [Figs. 2(a) and 2(d)] to realize stiffness adaptation [Fig. 2(f)] and a fast actuator u_2 to change the effective length of the second leaf spring x_2 [Figs. 2(a) and 2(d)] and as such implement stiffness pumping, i.e., fast modulation [Fig. 2(h)]. Unlike in the minimalistic model (1), the stiffness of this real system (8) is not directly controllable, and, as such, our previously derived composite controller (5) is not directly applicable. In general, finding the optimal control inputs $\boldsymbol{u}$ to realize a desired stiffness modulation, under realistic actuation [i.e., (7) and (8)], requires model-based computation [30]. However, if the oscillator's restoring force [i.e., (6); $-k(q,\boldsymbol{x})q$] is strictly monotonic with respect to the control inputs, one can formally replace the stiffness in (5) [Figs. 1(b) and 1(c)] with the control inputs in (7) to define a more general control law for nonlinear parametric excitation [23]:

$$\boldsymbol{u} = [u_o(\bar{q}_N, \bar{A}_N), u_p(q,\dot{q})]^\top \in [\boldsymbol{u}_{\min}, \boldsymbol{u}_{\max}]. \tag{9}$$

The design condition enabling this model and computation free generalization is satisfied on our device under static condition—due to the monotonic stiffness motor position relation, i.e., $\boldsymbol{u} \approx \boldsymbol{x}$, $\partial k/\partial x_1 > 0$, and $\partial k/\partial x_2 > 0$. This is sufficient to implement near-optimal parametric excitation using real (bandwidth limited) actuators. This holds not only for slow adaptation u_o but also for switching-like parameter modulation u_p, provided the oscillator is slow compared to the actuator performing the fast parameter modulation (i.e., the frequency of oscillations is an order of magnitude below the bandwidth of the fast stiffness modulating actuator [33]).

There are three important features that set this *redundantly actuated self-tuning bistable parametric feedback oscillator* apart from more conventionally actuated monostable oscillators:

First, instead of utilizing one actuation mechanism to realize fast parameter modulation in large stiffness range, the proposed device employs two actuated compliant mechanisms: one to enable slow temporal modulation in large stiffness range and another to realize fast temporal modulation in the small stiffness range. This redundancy in the actuation directly allows the oscillator to exploit the physical differences inherent to the tuning and pumping controllers. In particular, this enables low-power practical implementation of the proposed composite controller (9), see Figs. 2(g) and 2(i) and Fig. 3.

Second, in our device, stiffness modulation is realized with variable-length leaf-spring mechanisms which largely decouple the external load from the stiffness adjusting actuators. By doing so, the actuators do not need to work heavily when changing stiffness, and at the same time they require little power to maintain stiffness [31]. This actuation principle exemplifies a practical means to realize parametric excitation with low actuation power and energy cost, see Figs. 2(g) and 2(i) and Fig. 3.

Third, our device incorporates a negative stiffness mechanism that extends its mono-stable operation regime to strongly nonlinear bistable regimes [Fig. 2(e) and Fig. 4]. Instead of realizing adaptable positive feedback using energetically expensive active control (e.g., by changing the length of the large extension springs [Fig. 2(c) (III)] with a strong actuator), our implementation does not require any energy input to generate the positive feedback effect during the oscillations. Unlike time-dependent parametric excitation of monostable oscillators, this adaptive feedback-controlled negative stiffness system enables self-initialization [Figs. 2(e) and 2(f), B_1] and

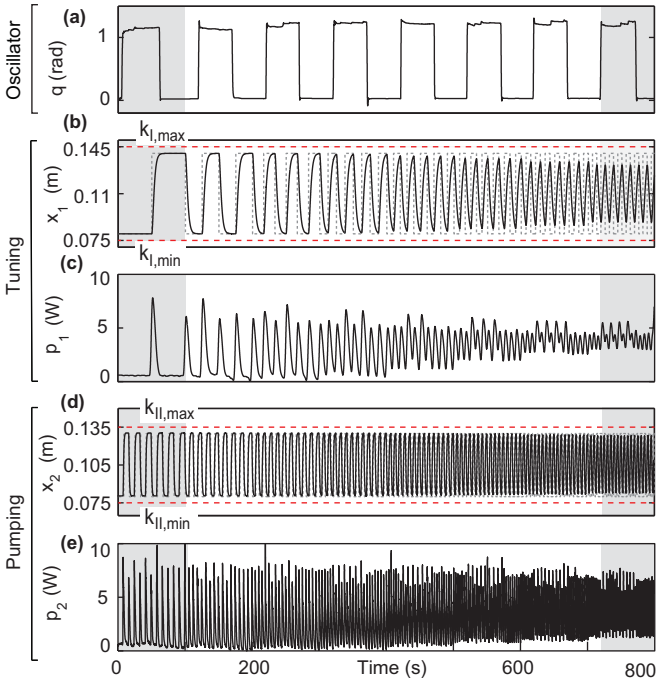

FIG. 3. Power drained for stiffness modulation. (a) Position of the oscillator [$q = 0$ (rad) indicates nondeflected configuration while $q \approx 1$ (rad) indicates the maximally deflected configuration during the experiments]. (b) Motion of the stiffness tuning actuator x_1 (solid black lines) and the corresponding square-wave input motor command u_1—chirp signal with frequency [0.01,0.08] Hz (dashed gray lines). (c) Average power drained by the stiffness tuning actuator (computed using a 2.5-s moving average filter). The plot shows no essential difference between the electrical motor power in the case when the oscillator was not deflected compared to the case when it was maximally deflected from its equilibrium configuration. This can be seen in the gray areas on the left. (d) Motion of the stiffness pumping actuator x_2 (solid black lines) given the square-wave input command u_2—chirp signal with frequency [0.06,0.2] Hz. (e) Average power drained by the stiffness pumping actuator (computed using a 0.25-s moving average filter). The plot shows small variation between the motor power in the case when the oscillator was not deflected compared to the case when it was maximally deflected from its equilibrium configuration. In both power plots there is a consistent up-shift of the baseline motor power due to the increased frequency of the excitation.

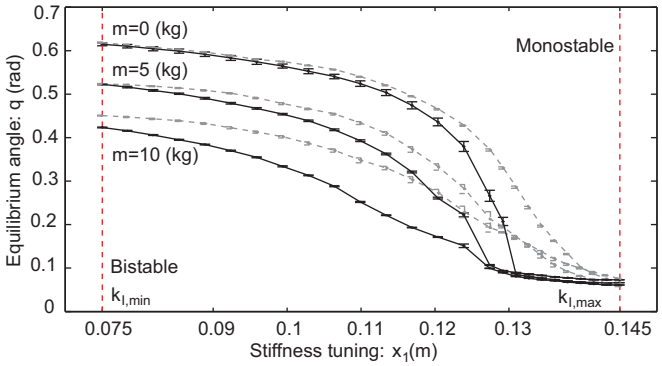

FIG. 4. Equilibrium angle of the oscillator as a function of its static stiffness setting. The gray (black) lines denote the equilibrium positions of the oscillator under quasistatic forward (and backward) sweep of the stiffness. During these experiments three different weights, i.e., $m = \{0,5,10\}$ kg were attached to the oscillator. The error bars on this plot denote two standard deviations. We observe that when the stiffness is tuned to its minimum value ($x_1 \approx x_{1\min}$) the trivial equilibrium of the system is unstable, the oscillator is bistable. When the stiffness is tuned to its maximum value ($x_1 \approx x_{1\max}$) the trivial equilibrium is stable, and the oscillator is monostable. In the monostable case, the oscillator has nonzero static deflection. This is due to symmetry-breaking terms in real-world implementation. The bifurcation phenomenon seen in this plot is enabled by the positive feedback (negative stiffness) extension spring mechanism in our device [Figs. 2(c) and 2(d) (III)].

large-amplitude resonant vibrations [Figs. 2(e) and 2(f), B_2] using small control perturbations [Figs. 2(e) and 2(h)].

V. DISCUSSION AND CONCLUDING REMARKS

A typical operation of the oscillator is shown in Figs. 5(a) and 5(b) (see also Movie 1 and Movie 2 provided in the Supplemental Material [34]). The effect of the tuning [Fig. 5(c)] can be identified by a long-term transient response that leads to large-amplitude vibrations [Fig. 5(b)]. The concurrent fast stiffness pumping [Fig. 5(e)] provides the energy input for sustained vibrations. The experiment shows unprecedented level of robustness, i.e., (1) self-tuning [Figs. 5(a) and 5(b)(A)], (2) quick recovery under large short-term perturbations [Figs. 5(a) and 5(b)(B)], (3) readaptation under long-term perturbations [Figs. 5(a) and 5(b)(F)], and (4) consistent retuning under significant modification of the parameters of the oscillator [Figs. 5(a) and 5(b)(C)–(D)]. None of these behaviors are preprogrammed, i.e., neither the model of the system nor the perturbations (provided by the experimenter) are used in any way to control the oscillator. The adaptation process was also tested by applying heavy damping and strong time-dependent external driving to the oscillator (Fig. 6). Despite these effects, the oscillator demonstrates robust readaptation [Figs. 6(b) and 6(c)] without model information or knowledge of the nonstationary excitation.

The operation of the oscillator can be decomposed to a slow long time-scale adaptation [Fig. 5(c) and Fig. 6(c)] and a fast but short time-scale feedback modulation [Fig. 5(e) and Fig. 6(e)]. The adaptation process is intermittent if there are no perturbations [Fig. 5(c)] and under stationary excitation [Fig. 6(c)]. In addition to this, once adapted, the oscillator can operate with low power to hold its stiffness setting [Figs. 5(d) and Fig. 6(d)]. As opposed to stiffness tuning, the concurrent fast parametric feedback pump is triggered twice per every oscillation cycle. This excitation is effective despite the small range of the corresponding position modulation x_2. This is because: (i) the oscillator is tuned to operate at the vicinity of its dynamic bifurcation (where it displays extreme sensitivity to parameter perturbations) but also because (ii) the oscillator employs near-optimal resonance perturbations. These effects can dramatically enhance the effect of parameter modulation [i.e., which in turn reduces the power required to maintain

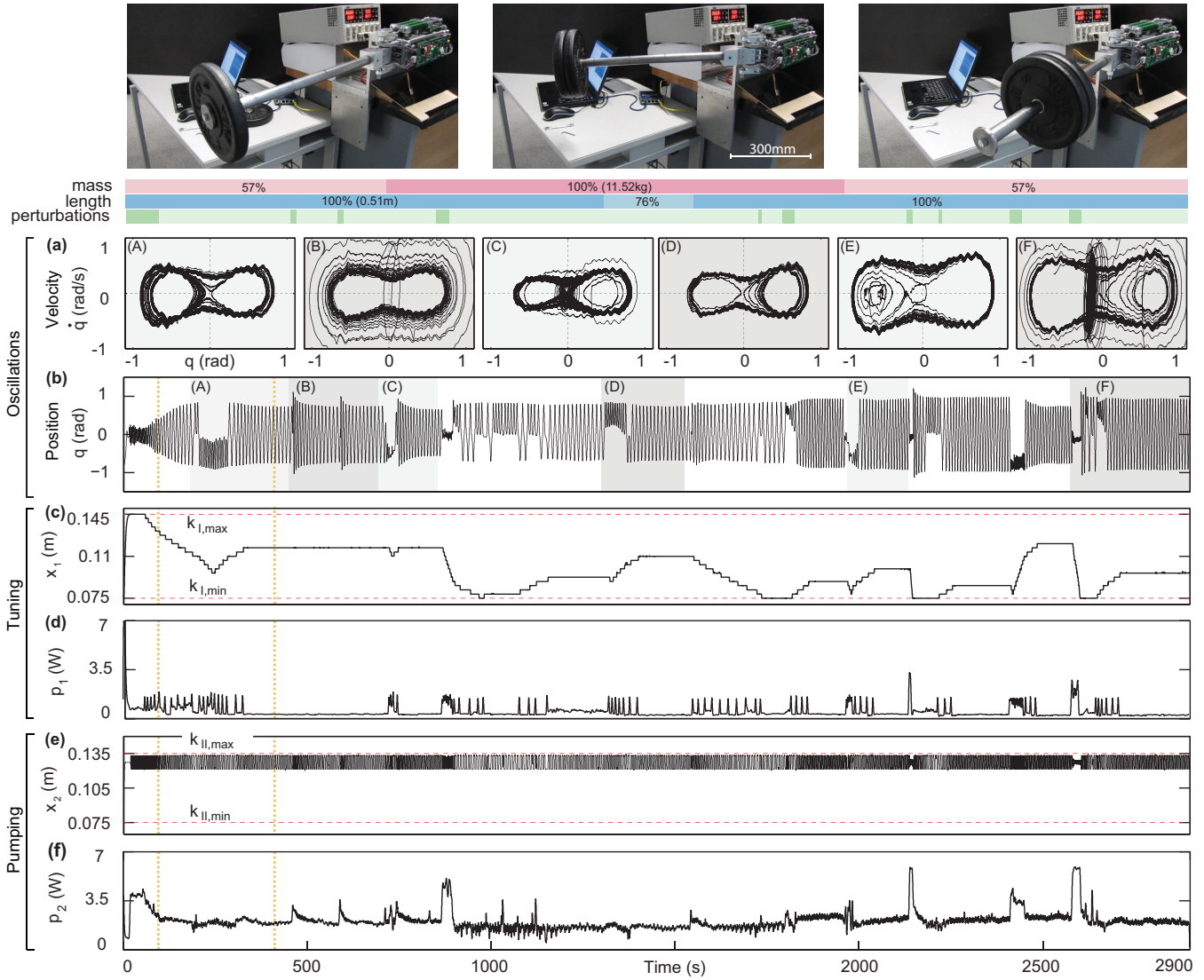

FIG. 5. Self-tuning parametric feedback oscillator. The first three pictures show the experimental setup. The color code on the top of the plot shows the mass and length of the equivalent mathematical pendulum [from left to right: $L_{eq} = \{0.51, 0.51, 0.39\}$ m and $m_{eq} = \{6.56, 11.52, 11.57\}$ kg respectively], and the duration of the perturbations imposed during the experiment. [(a) and (b)] Response of the oscillator under model variation and the imposed perturbations. The six insets (A)–(F) exemplify different modes of self-tuning. (c) Self-tuning—motion of the stiffness tuning actuator. (d) Power drained by the stiffness tuning actuator. (e) Motion of the actuator performing the fast feedback-based stiffness modulation. (f) Power drained by the actuator implementing the fast stiffness modulation. The operation of the actuators and the motion of the oscillator (between the dashed yellow lines) are shown in Movie 1 and Movie 2 of the Supplemental Material [34]. Additional experimental results are provided in the Appendix (Fig. 7).

sustained oscillations; Figs. 5(d) and 5(f) and Figs. 6(d) and 6(f)].

The ability of the oscillator to increase its sensitivity by self-tuning to the onset of bifurcation, is vital to realize large-amplitude motion with weak parameter modulation. However, self-tuning to critical transition is an effective means of signal amplification even without fast parameter modulation. Due to the generality, robustness, and minimal implementation requirement, the present tuning approach may be used to design active and adaptive sensors that, similarly to the human ear [35], could achieve unprecedented bandwidth and sensitivity in practical applications. In addition to this, we posit that efficient implementation of wide-range self-tuning, as the one demonstrated on our electromechanical oscillator, could enable adaptive realization of the celebrated stochastic resonance phenomenon [36] useful not only for signal amplification [37] but also for a variety of different applications, including adaptive energy harvesting from random natural vibrations [38].

Parametric excitation has been widely used for signal amplification [39] and frequency stabilization [8] in micro- and nanoelectromechanical oscillators. The high-quality factor (low dissipation) makes these devices inherently sensitive to parametric excitation. Also parametric actuation can be

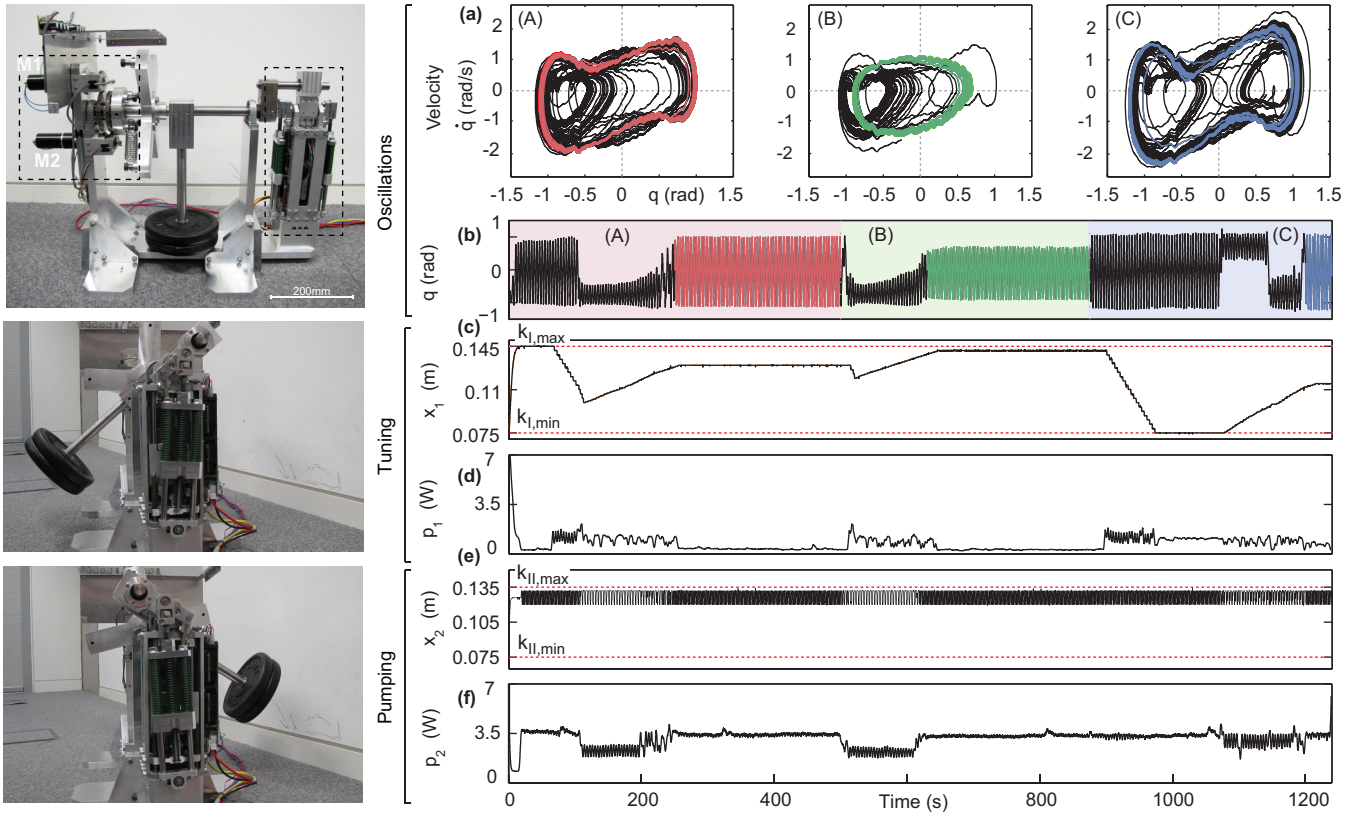

FIG. 6. Self-tuning oscillator under heavy damping and strong external excitation. The three pictures on the left show the device used to impose controlled damping and external torque on the oscillator. In the first picture, the box on the right shows the two driving motors (M1 and M2) while the box on the left shows the oscillator. The second and third pictures show the extreme left and the extreme right position of the oscillator, respectively. One of the motors (M1) on this device is used to impose a velocity-dependent damping torque while another (M2) is used to generate a time- and position-dependent driving torque. The red, blue, and green phases indicate (A) medium, (B) weak, and (C) strong external driving imposed by the torque generator. (a) Phase plots of the motion. The colored cycles show stationary oscillations following the adaptation. (b) Motion of the oscillator in time. (c) Stiffness adaptation. The strategy to first reduce stiffness, induce off-centered oscillations, and then increase stiffness, backtrack until large amplitude oscillations, is clearly observed during all three motion phases. (d) Average power for stiffness tuning. Regardless of the motion of the oscillator, the power required to maintain stiffness is near to the baseline power of the resting actuator. (e) Stiffness pumping. (f) Average power for stiffness pumping. While maintaining stiffness requires negligible energy on our system, the total energy cost for stiffness modulation is dominated by the speed of the stiffness pumping actuator, and it is significantly higher than the one required for stiffness adaptation.

realized using a universal transduction scheme for nanomechanical oscillators [40]. However, the effective use of micro- and nanodevices is in strongly nonlinear, large-amplitude, regimes where the classical principle of time-dependent parametric excitation suffers from frequency detuning and amplitude saturation even under no dissipation.

The present finding provides robust, model-free, and near-optimal parametric excitation using judiciously chosen feedback perturbations. Application of this principle could lead to new-generation self-tuning bistable parametric oscillators that provide near-optimal amplitude maximization and is robust to variability in fabrication, nonlinearity in operation, imperfections in actuation, and uncertain external effects inevitably present in real-world implementation.

ACKNOWLEDGMENTS

This work was supported by the first author's Start-up Research Grant No. SRG-EPD-2014-074 at the Singapore University of Technology and Design and the author's Initiating Knowledge Transfer Grant No. IKTF 10P-12/0963 at the University of Edinburgh. The authors also acknowledge the contribution of Vladimir Ivan (University of Edinburgh) for his work on the software control interface.

APPENDIX

Figure 7 provides additional experimental results. These results demonstrate the behavior of the oscillator under substantial model variation.

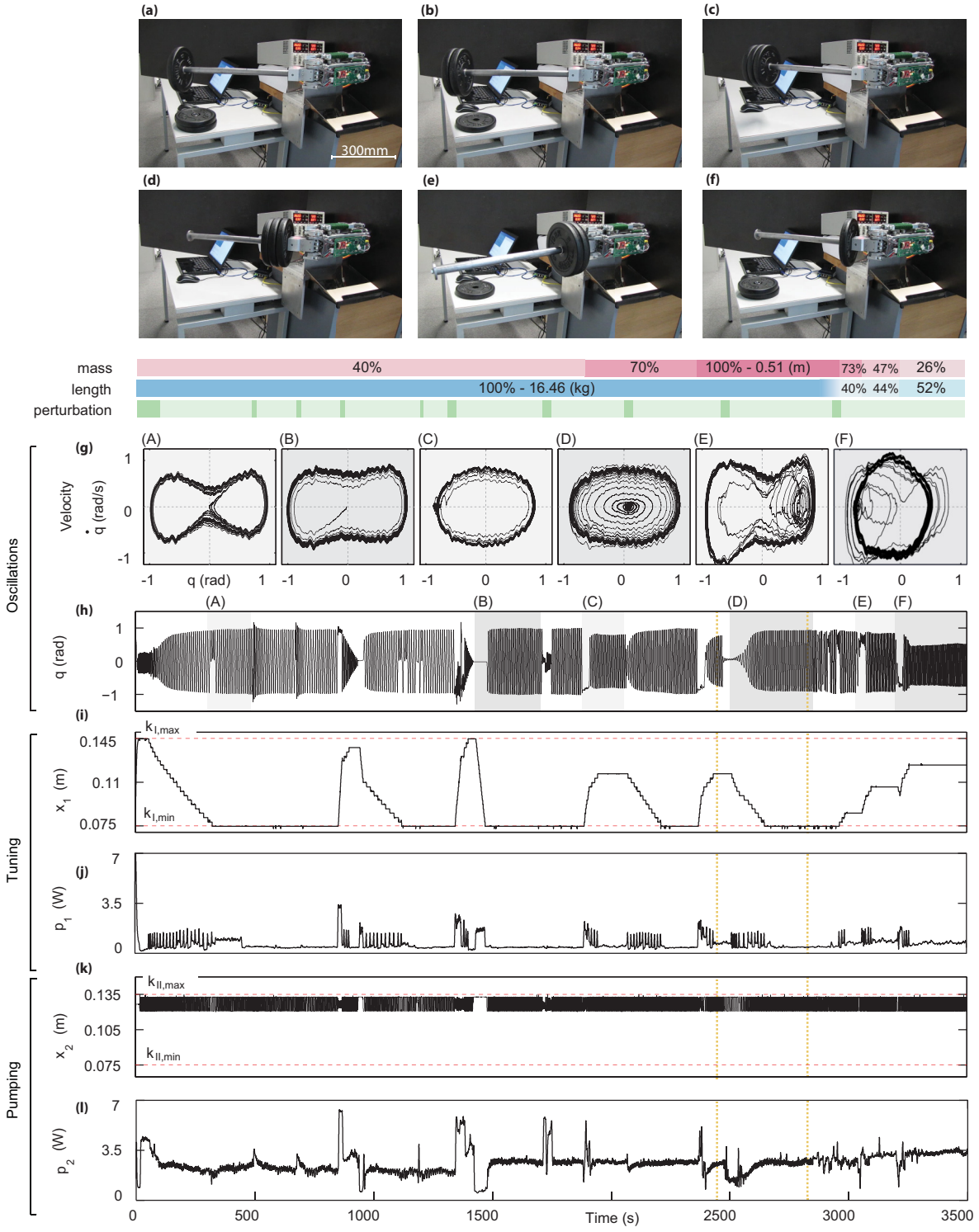

FIG. 7. Self-tuning parametric feedback oscillator. [(a)–(f)] The plots show the structural changes imposed to the oscillator during the experiment. The parameters, length L_{eq}, and mass m_{eq} of the equivalent mathematical pendulum, representing this system, are given by (a) $L_{eq} = 0.51$ m, $m_{eq} = 6.56$ kg; (b) $L_{eq} = 0.51$ m, $m_{eq} = 11.52$ kg; (c) $L_{eq} = 0.51$ m, $m_{eq} = 16.46$ kg; (d) $L_{eq} = 0.21$ m, $m_{eq} = 12.21$ kg; (e) $L_{eq} = 0.22$ m, $m_{eq} = 7.79$ kg; and (f) $L_{eq} = 0.27$ m, $m_{eq} = 4.25$ kg, respectively. The changes in the system parameters are indicated by the red-blue color code. [(g) and (h)] Response of the oscillator under model variation and the imposed perturbations described in the event code on the top of the plot. The six insets (A)–(F) exemplify different means of self-tuning. Notably, insets (B) and (D) show self-initialization of the oscillations. This is shown in Movie 3, which demonstrates the motion of the oscillator between the dashed yellow lines. [(i) and (j)] Self-tuning—motion and power drained by the stiffness tuning actuator. [(k) and (l)] Stiffness pumping—motion and power drained due to the fast stiffness modulation. The plots show unprecedented level of robustness under significant changes of the mechanical properties of the oscillator.

[1] M. Faraday, Philos. Trans. R. Soc. London **121**, 299 (1831).
[2] F. Melde, Ann. Phys. Chem. **109**, 193 (1859).
[3] J. R. Sanmartín, Am. J. Phys. **52**, 937 (1984).
[4] K. L. Turner, S. A. Miller, P. G. Hartwell, N. C. MacDonald, S. H. Strogatz, and S. G. Adams, Nature **396**, 149 (1998).
[5] D. Rugar and P. Grütter, Phys. Rev. Lett. **67**, 699 (1991).
[6] W. Paul, Rev. Mod. Phys. **62**, 531 (1990).
[7] C. Macklin, K. O'Brien, D. Hover, M. E. Schwartz, V. Bolkhovsky, X. Zhang, W. D. Oliver, and I. Siddiqi, Science **350**, 307 (2015).
[8] L. G. Villanueva, R. B. Karabalin, M. H. Matheny, E. Kenig, M. C. Cross, and M. L. Roukes, Nano Lett. **11**, 5054 (2011).
[9] A. Marandi, Z. Wang, K. Takata, R. L. Byer, and Y. Yamamoto, Nat. Photon. **8**, 937 (2014).
[10] S.-B. Shim, M. Imboden, and P. Mohanty, Science **316**, 95 (2007).
[11] S. C. Masmanidis, R. B. Karabalin, I. De Vlaminck, G. Borghs, M. R. Freeman, and M. L. Roukes, Science **317**, 780 (2007).
[12] É. Mathieu, J. Math. Pures Appl. **13**, 137 (1868).
[13] A. Stephenson, Q. J. Pure Appl. Math. **37**, 353 (1906).
[14] B. van de Pol and M. J. O. Strutt, Philos. Mag. **5**, 18 (1928).
[15] L. Rayleigh, Philos. Mag. **15**, 229 (1883).
[16] L. I. Mandelstam and N. D. Papaleksi, Z. Teknich. Fiz. **4**, 5 (1934).
[17] A. Nayfeh and D. Mook, *Nonlinear Oscillations* (Wiley-Interscience, New York, 1979).
[18] D. Ramos, J. Mertens, M. Calleja, and J. Tamayo, Appl. Phys. Lett. **92**, 173108 (2008).
[19] R. van Leeuwen, D. M. Karabacak, S. H. Brongersma, M. Crego-Calama, H. S. J. van der Zant, and W. J. Venstra, Microelectron. Eng. **98**, 463 (2012).
[20] J. Gieseler, B. Deutsch, R. Quidant, and L. Novotny, Phys. Rev. Lett. **109**, 103603 (2012).
[21] A. Pikovsky, M. Rosenblum, and J. Kurths, *Synchronization: A Universal Concept in Nonlinear Sciences* (Cambridge University Press, Cambridge, 2001).
[22] K. Wiesenfeld and B. McNamara, Phys. Rev. Lett. **55**, 13 (1985).
[23] D. J. Braun, Phys. Rev. Lett. **116**, 044102 (2016).
[24] G. Duffing, *Erzwungene Schwingungen bei Veränderlicher Eigenfrequenz und ihre technische Bedeutung* (F. Vieweg & Sohn, Braunschweig, 1918).
[25] E. Meissner, Schweiz. Bauz. **72**, 95 (1918).
[26] The three parameters of the tuning controller provide the means to increase the robustness of the excitation. However, there is a trade-off between amplitude maximization and the robustness of the tuned oscillator, i.e., the closer the system is to bifurcation, the higher the amplitude of the oscillations, but the appearance of irregular oscillations (switching between off-centered small amplitude oscillations and centered large amplitude oscillations) is more likely, in this case, under external perturbations.
[27] M. Scheffer, J. Bascompte, W. A. Brock, V. Brovkin, S. R. Carpenter, V. Dakos, H. Held, E. H. van Nes, M. Rietkerk, and G. Sugihara, Nature **461**, 53 (2009).
[28] N. Minorsky, J. Appl. Phys. **22**, 49 (1951).
[29] A. Fradkov, Physica D **128**, 159 (1999).
[30] D. J. Braun, F. Petit, F. Huber, S. Haddadin, P. van der Smagt, A. Albu-Schäffer, and S. Vijayakumar, IEEE Trans. Robot. **29**, 1085 (2013).
[31] D. J. Braun, S. Apte, O. Adiyatov, A. Dahiya, and N. Hogan, *IEEE International Conference on Robotics and Automation (ICRA), Stockholm, Sweden* (IEEE, Piscataway, 2016), pp. 636–641.
[32] Due to real-world effects, including friction and nonlinearities in the actuation, identifying a model that can quantitatively predict long-term behavior of this device turned out to be nontrivial. This is typical in nonlinear systems, i.e., oscillators exhibiting large-amplitude motion, and the main reason why finding the optimal control inputs is elusive by using model-based optimization.
[33] The higher the bandwidth of stiffness modulation compared to the frequency of the oscillations, the more closely the proposed feedback excitation can approximate the optimal parametric feedback excitation.
[34] See the Supplemental Movies at http://link.aps.org/supplemental/10.1103/PhysRevE.95.012201 for three supplemental Movies that demonstrate the principle of self-tuning parametric feedback excitation and show the robustness of the oscillator.
[35] S. Camalet, T. Duke, F. Jülicher, and J. Prost, Proc. Natl. Acad. Sci. USA **97**, 3183 (2000).
[36] L. Gammaitoni, P. Hänggi, P. Jung, and F. Marchesoni, Rev. Mod. Phys. **70**, 223 (1998).
[37] R. L. Badzey and P. Mohanty, Nature **437**, 995 (2005).
[38] F. Cottone, H. Vocca, and L. Gammaitoni, Phys. Rev. Lett. **102**, 080601 (2009).
[39] R. B. Karabalin, R. Lifshitz, M. C. Cross, M. H. Matheny, S. C. Masmanidis, and M. L. Roukes, Phys. Rev. Lett. **106**, 094102 (2011).
[40] Q. P. Unterreithmeier, E. M. Weig, and J. P. Kotthaus, Nature **458**, 1001 (2009).